Soft Matter

Multi-Energy Dissipation Mechanisms in Supramolecular Hydrogels with Fast and Slow Relaxation Modes

Journal:	*Soft Matter*
Manuscript ID	SM-ART-06-2022-000735.R1
Article Type:	Paper
Date Submitted by the Author:	19-Aug-2022

Complete List of Authors:	Konishi, Subaru; Osaka University Graduate School of Science Department of Macromolecular Science Park, Junsu; Graduate School of Science, Osaka University, Department of Macromolecular Science Urakawa, Osamu; Osaka University, Department of Molecular Science Osaki, Motofumi; Graduate School of Science, Osaka University, Department of Macromolecular Science Yamaguchi, Hiroyasu; Osaka University, Department of Macromolecular Science, Graduate School of Science Harada, Akira; Osaka University Graduate School of Science Department of Macromolecular Science, Inoue, Tadashi; Osaka University, Macromolecular Science Matsuba, Go; Yamagata University, Takashima, Yoshinori; Graduate School of Science, Osaka University, Department of Macromolecular Science; Institute for Advanced Co-Creation Studies,

ARTICLE

Multi-Energy Dissipation Mechanisms in Supramolecular Hydrogels with Fast and Slow Relaxation Modes

Received 00th January 20xx,
Accepted 00th January 20xx

DOI: 10.1039/x0xx00000x

Subaru Konishi,[a] Junsu Park,[a,c], Osamu Urakawa,[a] Motofumi Osaki,[a,c] Hiroyasu Yamaguchi,[a,c,d] Akira Harada,[e] Tadashi Inoue,[a,c] Go Matsuba,*[f] and Yoshinori Takashima*[a,b,c,d]

Reversible cross-links by non-covalent bonds have been widely used to produce supramolecular hydrogels that are both tough and functional. While various supramolecular hydrogels with several kinds of reversible cross-links have been designed for many years, a universal design that would allow control of mechanical and functional properties remains unavailable. The physical properties of reversible cross-links are usually quantified by thermodynamics, dynamics, and bond energies. Herein, we investigated the relation between the molecular mobility and mechanical toughness of supramolecular hydrogels consisting of two kinetically distinct reversible cross-links by host-guest interactions. The molecular mobility was quantified as the second-order average relaxation time ($<\tau>_w$) of the reversible cross-links. We discovered that hydrogels combining fast ($<\tau>_w$ = 1.8 or 18 s) and slowly ($<\tau>_w$ = 6.6×10^3 or 9.5×10^3 s) reversible cross-links showed increased toughness compared to hydrogels with only one type of cross-link because relaxation processes in the former occurred with wide timescales.

1. Introduction

Tuning the chemical and physical properties of polymeric materials is an important issue for widespread application, long service life, resource reduction, processability, and functionalization such as responsiveness, self-healing, and excellent mechanical properties.[1–11] In particular, the mechanical performance of synthetic hydrogels[12,13] is usually weaker than those of elastomers and natural hydrogels,[14–16] which limits their broad application.[15,17] To achieve tough materials, mechanisms for dissipating energy from the environment or approximating an ideal polymer network are needed.[7,18–28] One effective approach is to introduce reversible cross-links, such as non-covalent[29,30] or dynamic covalent bonds[31], into polymeric materials. They can dissociate when a polymeric material is under mechanical stress. The dissociation relaxes the stretched polymer chains and leads to dissipation of energy from the polymer network, high stretchability of the polymer network, and eventually toughening of the materials.[18]

The characteristics of non-covalent bonds are often quantified by thermodynamics and dynamics.[21,29,32,33] These parameters complexly tune the properties of cross-linked supramolecular polymeric materials. In general, the thermodynamic parameter will relate to the degree of cross-linking in the network. The dynamics parameter directly influences the dynamic nature of cross-links and surrounding polymer chains, which will determine macroscopic viscoelasticity. Therefore, the dynamics of non-covalent bonds will affect the timescale of the above energy dissipation mechanism by reversible cross-links.

Inspired by the different features of non-covalent bonds, combinations of several kinds of reversible cross-links in a single network have attracted much attention as a way to establish more highly functional materials.[32] Such hydrogels containing two kinds of reversible cross-links are called dual physically cross-linked hydrogels. While many of them were designed for effective self-healing[34–37] and multi-stimuli responsiveness[38–44], some hydrogels cross-linked by metal-ligand coordination[33,45], hydrogen bonding[46,47], or ionic interactions[48,49] have exhibited outstanding mechanical properties, probably due to their high binding energies.[34,50–55] For diverse hydrogels as well as dual physically cross-linked hydrogels, there is no known set of general principles with which to design properties and functionality.[18,24,56,57]

In addition, different reversible cross-links usually associate and dissociate with different timescales.[58–67] Therefore, a combination of different reversible cross-links also influences the viscoelastic properties of dual physically cross-linked hydrogels, where the dynamics of reversible cross-links with different timescales may produce a specific response to the external deformation.[68–72] Although the dynamics should be

[a] Department of Macromolecular Science, Graduate School of Science, Osaka University, 1-1 Machikaneyama, Toyonaka, Osaka 560-0043 Japan. E-mail: takasima@chem.sci.osaka-u.ac.jp
[b] Institute for Advanced Co-Creation Studies, Osaka University, 2-1 Yamada-oka, Suita, Osaka 565-0871 Japan.
[c] Forefront Research Center, Osaka University, 1-1 Machikaneyama, Toyonaka, Osaka 560-0043 Japan.
[d] Institute for Open and Transdisciplinary Research Initiatives, Osaka University, 2-1 Yamada-oka, Suita, Osaka 565-0871 Japan.
[e] SANKEN (The Institute of Scientific and Industrial Research), Osaka University, 8-1 Mihogaoka, Ibaraki, Osaka 567-0047 Japan.
[f] Graduate School of Organic Material Engineering, Yamagata University, 4-3-16 Jonan, Yonezawa, Yamagata 992-8510, Japan. E-mail: gmatsuba@yz.yamagata-u.ac.jp
†Electronic Supplementary Information (ESI) available: See DOI: 10.1039/x0xx00000x

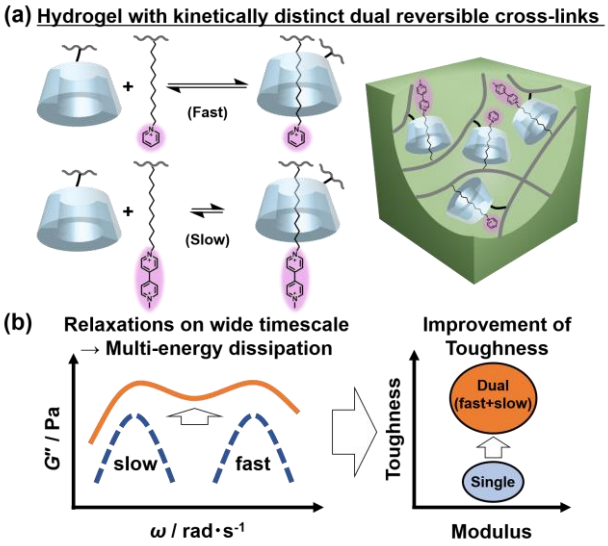

Fig. 1. Conceptual figure for the present work. **(a)** Schematic of a supramolecular hydrogel with two reversible cross-links exhibiting distinct kinetics. **(b)** Schematics for viscoelastic relaxation of the supramolecular hydrogels and the corresponding high toughness.

related to the energy dissipation mechanisms and toughness of the hydrogels, only a few studies on the quantitative relationships between dynamics and toughness have been reported.[25,65,67,73–79]

Herein, we show the relation between a combination of different molecular mobility and toughness values for supramolecular hydrogels (**Fig. 1**). To do this, we prepared hydrogels with dual reversible cross-links by using host-guest complexation of α-cyclodextrins (αCDs) and cation-terminated alkyl chain guests. We focused on the viscoelastic relaxation time (τ) as a parameter for the molecular mobility of reversible cross-links. τ is defined as the characteristic time required for the modulus or stress to decrease to the value divided by Napier's constant under stress. Therefore, it will be useful for the discussion of energy dissipation in polymer materials as it closely relates to mechanical phenomena. Depending on the structure of the host-guest complex and the kinetics of bond breaking, the reversible cross-links show distinct second-order average relaxation times ($<\tau>_w$).[65] Previously, in the case of the hydrogel with one type of reversible cross-link, we demonstrated the balance between $<\tau>_w$ and initial strain rate was important to improve toughness. By contrast, supramolecular hydrogels consisting of two different host-guest cross-links are expected to show unique relaxation behavior on wide timescales. We investigated the effects of combined reversible cross-links with different $<\tau>_w$ values on the viscoelastic and the mechanical properties of supramolecular hydrogels to design an effective energy dissipation mechanism.

2. Experimental

Materials and Measurements are described in Electronic Supplementary Information (ESI).

Preparation of the αCD-R_1-R_2 hydrogels

The αCD-R_1-R_2 (2, 1, 1) and αCD-R (2, 2) hydrogels were prepared by radical copolymerization with a redox initiator system according to our previous reports[64,65,80]. **Fig. 2c** shows a typical polymerization scheme for the former hydrogels. The αCD monomer (αCDAAmMe) and two guest monomers with different cation end groups (R monomers) were sonicated in a 0.5 M potassium chloride (KCl) solution at 50 °C for one hour to form two different 1:1 inclusion complexes. Because the K_a values of the R monomers and their molar concentrations were almost the same, each R_1 and R_2 monomers could form similar amounts of complexes with αCDAAmMe. The acrylamide (AAm) main monomer and potassium persulfate (KPS) were added to the resulting solution. Then, the total concentration of monomers was set to 2 M. The molar ratios of αCDAAmMe, R_1, R_2, AAm, and KPS were 2.0, 1.0, 1.0, 96 and 1.0 mol%, respectively. Finally, 1.0 mol% of *N*,*N*,*N*′,*N*′-tetramethylethylenediamine (TEMED) was added. The solution was shaken quickly and poured into a Teflon mold to start gelation. Details of the reagents and solutions are presented in the Supplementary Information (**Scheme S1 and Tables S1–S15**). The αCD-R_1-R_2 (2, 1, 1) hydrogels containing VC11 were light yellow and transparent, and the others were colorless and transparent.

3. Results

3-1. Characteristics of the αCD-R_1-R_2 hydrogels

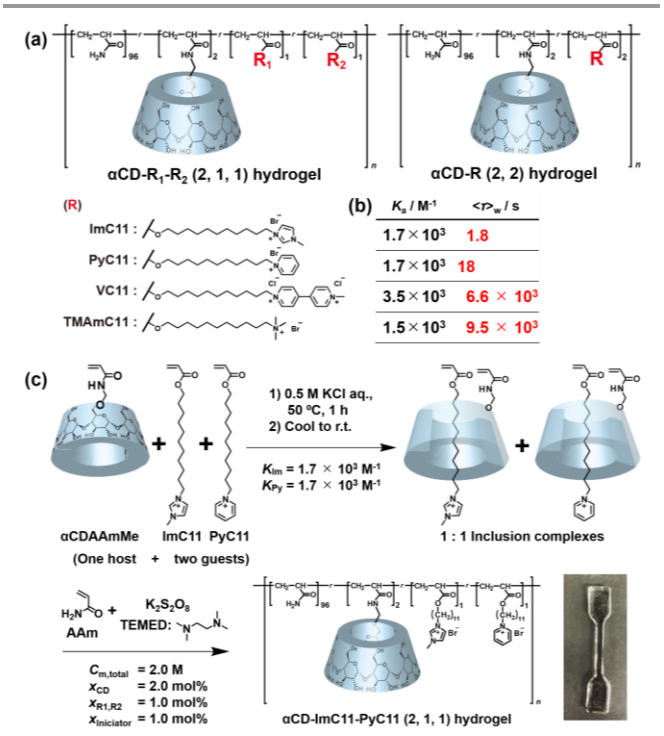

Fig. 2. (a) Chemical structures of the αCD-R_1-R_2 (2, 1, 1) and αCD-R (2, 2) hydrogels. **(b)** Association constant (K_a) of αCDAAmMe with cation-terminated alkyl (R) monomers and the second-order average relaxation time ($<\tau>_w$) of the corresponding αCD-R crosslink. K_a was measured in previous studies.[64,65,95] **(c)** Typical preparation scheme and a picture of the αCD-ImC11-PyC11 (2, 1, 1) hydrogel. Other αCD-R_1-R_2 (2, 1, 1) and αCD-R (2, 2) hydrogels were prepared in a similar way.

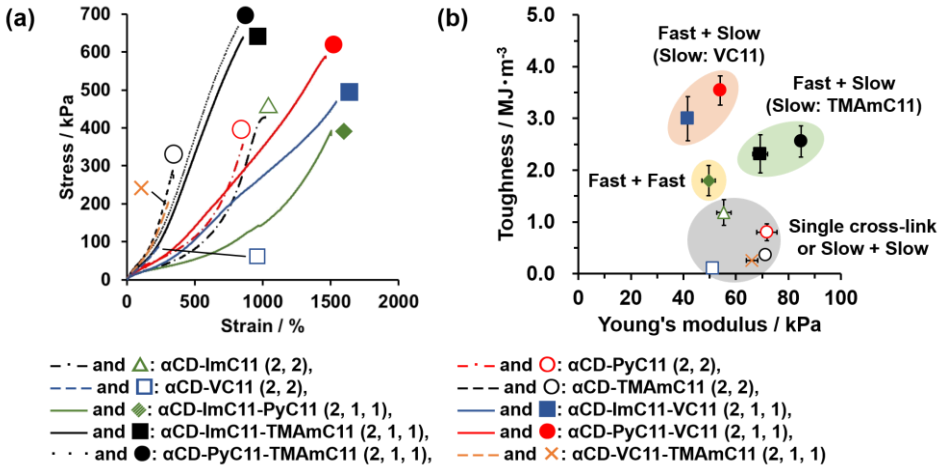

Fig. 3. Mechanical properties of the αCD-R_1-R_2 (2, 1, 1) and αCD-R (2, 2) hydrogels. **(a)** Stress–strain curves. **(b)** Plots of toughness and Young's modulus. αCD-ImC11 (2, 2): black chain line and green open triangle (△). αCD-PyC11 (2, 2): red chain line and red open circle (○). αCD-VC11 (2, 2): blue dashed line and blue open square (□). αCD-TMAmC11: black dashed line and black open circle (○). αCD-ImC11-PyC11 (2, 1, 1): green solid line and green filled diamond (◆). αCD-ImC11-VC11 (2, 1, 1): blue solid line and blue filled square (■). αCD-ImC11-TMAmC11 (2, 1, 1): black solid line and black filled square (■). αCD-PyC11-VC11 (2, 1, 1): red solid line and red filled circle (●). αCD-PyC11-TMAmC11 (2, 1, 1): black dotted line and black filled circle (●). αCD-VC11-TMAmC11 (2, 1, 1): orange dashed line and orange cross mark (×).

We prepared supramolecular hydrogels with dual or single reversible cross-links based on host-guest complexation between αCD (host) and various cation-terminated alkyl chains (guest molecules, R). The hydrogels with dual reversible cross-links were named αCD-R_1-R_2 (2, 1, 1) hydrogels (**Fig. 2a**). They have a poly(acrylamide) main chain and two kinds of host-guest units in the polymer side chains. (2, 1, 1) denotes the feed molar ratio of αCD, R_1, and R_2 units, respectively. Those with one type of host-guest cross-link, named αCD-R (2, 2) hydrogels, were prepared according to our previous work.[65]

The αCDs can include the linear alkyl chains in their cavities to form 1:1 inclusion complexes,[81,82] which act as reversible cross-links in the supramolecular hydrogels.[83–87] In contrast, cations have difficulty forming the inclusion complex directly due to electrostatic instability toward CDs but can also pass through the cavity of an αCD.[88,89] Therefore, cations at the alkyl end slow the kinetics for reactions of host-guest complexes of αCD with alkyl chains,[90,91] which leads to longer relaxation times (τ) for the αCD-R cross-links.[65] Furthermore, the high electric charge and bulkiness of cations make the τ values of the αCD-R cross-links longer. We prepared four kinds of cation-terminated alkyl monomers, ImC11, PyC11, VC11, and TMAmC11 (**Fig. 2a**). They have undecyl guest units and four different cationic units at the terminal imidazole (Im), pyridine (Py), viologen (V) and trimethylammonium (TMAm) groups. Their association constants (K_a) with αCDAAmMe monomers in aqueous solutions and the second-order average relaxation times ($\langle\tau\rangle_w$) of the corresponding αCD-R cross-links in the αCD-R (2, 2) hydrogels are summarized in **Fig. 2b**. Because dissociations of the αCD-R cross-links show several relaxation modes,[65] we simply use $\langle\tau\rangle_w$ to explain the difference in dynamics for each αCD-R cross-link. $\langle\tau\rangle_w$ is the average value of τ determined by considering the values of relaxation strength (G) and τ (eq. (6) in the Supplementary Information). While the values of K_a were almost the same, those of $\langle\tau\rangle_w$ varied depending on the structures of the cations. $\langle\tau\rangle_w$ for the αCD-ImC11 and αCD-PyC11 cross-links, which bore monocationic units, were relatively short at 1.8 and 18 s. When dicationic VC11 or bulky monocationic TMAmC11 was used, however, $\langle\tau\rangle_w$ for the αCD-VC11 and αCD-TMAmC11 cross-links were extraordinarily long at 6.6×10^3 and 9.5×10^3 s, respectively.

The as-prepared hydrogels were evaluated with tensile and rheological tests in this study, and hydrogels washed with D_2O were analyzed by IR and NMR spectroscopy (**Fig. S1–S13**). All of the units were confirmed from the IR and NMR spectra. Furthermore, the molar ratios of each unit were calculated from the FG-MAS NMR spectra. Their values were almost identical to the feed molar ratios, indicating that predefined molar ratios were introduced into the αCD-R_1-R_2 (2, 1, 1) hydrogels.

To confirm the formation of inclusion complexes serving as cross-links in the αCD-R_1-R_2 (2, 1, 1) hydrogels, we analyzed the hydrogels swollen in D_2O by 2-dimensional nuclear Overhauser effect spectroscopy (2D NOESY) (**Fig. S8–S13**). In all spectra, the protons of undecyl units showed NOE correlations to inner protons ($C^{3,5,6}H$) of the αCD units. This result indicates that the alkyl chains of R guests were included in the cavity of αCD and formed reversible cross-links in the hydrogels.

3-2. Mechanical properties of the αCD-R_1-R_2 hydrogels

The mechanical properties of the αCD-R_1-R_2 (2, 1, 1) and αCD-R (2, 2) hydrogels were evaluated with uniaxial tensile tests (tensile speed = 1.0 mm/s, room temperature = approximately 25 °C) (**Fig. 3a and S14–S19**). We calculated toughness by integrating the obtained stress-strain curves and Young's modulus from the initial slope of the curves. **Fig. 3b** shows the plots of toughness and Young's modulus. The toughness values varied with the structures of the reversible cross-links, while Young's moduli were almost the same. In particular, four of the hydrogels, the αCD-ImC11-VC11 (2, 1, 1), αCD-ImC11-TMAmC11 (2, 1, 1), αCD-PyC11-VC11 (2, 1, 1) and αCD-PyC11-TMAmC11 (2, 1, 1) hydrogels, showed relatively high toughness values (2.3~3.5 MJ/m³). The hydrogels consisted of

combinations of reversible cross-links with short $<\tau>_w$ of 1~10 s and long $<\tau>_w$ of > 1000 s. In particular, the toughness of the αCD-PyC11-VC11 (2, 1, 1) hydrogel (3.5 MJ/m^3) was 3-4 times larger than those of the αCD-PyC11 (2, 2) and αCD-VC11 (2, 2) hydrogels (0.80 and 0.10 MJ/m^3, respectively). On the other hand, in the case of the αCD-ImC11-PyC11 (2, 1, 1) hydrogel containing two fast reversible cross-links, the toughness was moderate (1.8 MJ/m^3). The αCD-VC11-TMAmC11 (2, 1, 1) hydrogel with two slowly reversible cross-links was weak (0.26 MJ/m^3). It was revealed that a combination of fast and slowly reversible cross-links significantly improved toughness while maintaining Young's modulus.

3-3. Linear viscoelasticity of the αCD-R_1-R_2 hydrogels

Dynamic viscoelastic measurements and stress-relaxation tests were performed to evaluate how the combination of reversible cross-links affected the relaxation behaviors of the αCD-R_1-R_2 (2, 1, 1) hydrogels (**Fig. S28–S33**). **Fig. S29d–S34d** show the master curves for the hydrogels referenced to 25 °C, and **Fig. S29f–S34f** show their stress-relaxation curves for 25 °C.

Fig. 4 shows a comparison of the αCD-PyC11-VC11 (2, 1, 1), αCD-PyC11 (2, 2) and αCD-VC11 (2, 2) hydrogels. According to our previous work[65,92], viscoelasticity of the αCD-R_1-R_2 (2, 1, 1) hydrogels αCD-R (2, 2) hydrogels can be explained by the stick reptation model.[93] Storage moduli (G') of the hydrogels show rubbery plateaus originating from the network formed by αCD-R cross-links in high angular frequency (ω) region. In the low ω (or long time) region where the cross-links dissociate, G' reduces to the second plateau derived from entanglements through the Rouse mode. Note that the terminal relaxation of chain reptation is not observed in the present experimental window because the cross-links retard the reptation process.

In the master curves (**Fig. 4b**), the αCD-PyC11-VC11 (2, 1, 1) and αCD-PyC11 (2, 2) hydrogels showed similar relaxation modes at $\omega = 10^{-1}$~10^{0} rad/s derived from αCD-PyC11 cross-links, while the αCD-VC11 (2, 2) hydrogel did not show relaxation in this ω range. In stress-relaxation curves (**Fig. 4c**), the αCD-PyC11-VC11 (2, 1, 1) hydrogel showed gradual relaxation similar

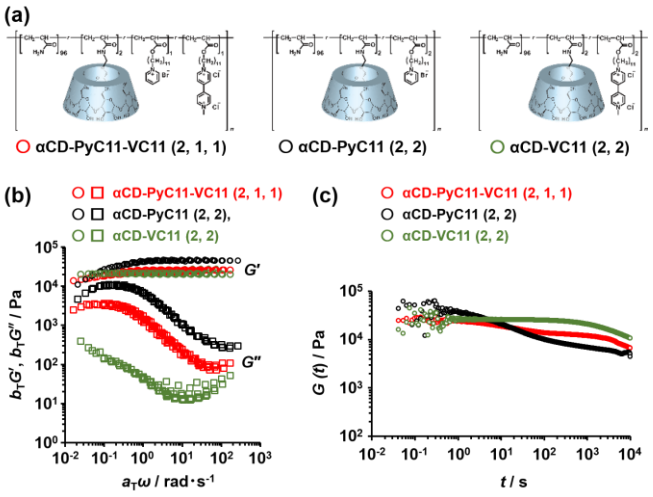

Fig. 4. Representative viscoelastic characteristics of the αCD-R_1-R_2 (2, 1, 1) and αCD-R (2, 2) hydrogels. **(a)** Chemical structures of the αCD-PyC11-VC11 (2, 1, 1), αCD-PyC11 (2, 2) and αCD-VC11 (2, 2) hydrogels. **(b)** Comparison of the master curves referenced at 25 °C. **(c)** Comparison of stress-relaxation curves at 25 °C.

to that of the αCD-PyC11 (2, 2) hydrogel in the short time region (~up to 100 s), whereas it showed a plateau and slower relaxation mode similar to those of the αCD-VC11 (2, 2) hydrogel in a long time (10^3~10^4 s) region. These results indicated that the αCD-PyC11-VC11 (2, 1, 1) hydrogel had combined relaxation modes derived from each network comprising αCD-PyC11 and αCD-VC11 cross-links. In other words, relaxation of each αCD-R cross-links in the αCD-PyC11-VC11 (2, 1, 1) hydrogel should occur independently.

To discuss the details, these master curves and relaxation curves were analyzed with the generalized Maxwell model (**Tables S16–S26**). **Table 1** shows the combined results for the relaxation modes calculated from both curves. In this section, we discuss τ and G of the individual relaxation modes but not $<\tau>_w$ because a comparison of individual relaxation modes is enough to examine the combined effects of the αCD-R cross-links on the relaxation behaviors of the αCD-R_1-R_2 (2, 1, 1) hydrogels. As shown in **Table 1**, for example, the αCD-PyC11-

Table 1. Relaxation strength (G_p), relaxation time (τ_p) in the p^{th} relaxation mode and terminal modulus (G_N) used for curve fitting of the αCD-R_1-R_2 (2, 1, 1) and αCD-R (2, 2) hydrogels.

Sample	G_1, τ_1 [Pa], [s]	G_2, τ_2 [Pa], [s]	G_3, τ_3 [Pa], [s]	G_4, τ_4 [Pa], [s]	G_5, τ_5 [Pa], [s]	G_N [Pa]
αCD-ImC11 (2, 2)	1.4×10^4, 0.09	1.5×10^4, 1.6	3.4×10^3, 11	1.3×10^3, 1.2×10^2	5.2×10^2, 3.3×10^3	9.5×10^3
αCD-PyC11 (2, 2)	-	1.4×10^4, 2.2	2.3×10^4, 19	4.1×10^3, 1.6×10^2	2.7×10^3, 2.4×10^3	5.2×10^3
αCD-VC11 (2, 2)	-	-	-	4.7×10^3, 1.0×10^3	1.2×10^4, 5.5×10^3	8.7×10^3
αCD-TMAmC11 (2, 2)	-	-	-	-	1.7×10^4, 9.5×10^3	0
αCD-ImC11-PyC11 (2, 1, 1)	7.3×10^3, 0.16	1.3×10^4, 2.4	1.1×10^4, 21	3.5×10^3, 1.9×10^2	1.9×10^3, 2.4×10^3	5.4×10^3
αCD-ImC11-VC11 (2, 1, 1)	6.0×10^3, 0.16	7.9×10^3, 2.9	1.0×10^3, 27	-	7.0×10^3, 4.6×10^3	8.7×10^3
αCD-ImC11-TMAmC11 (2, 1, 1)	6.3×10^3, 0.16	8.2×10^3, 2.4	-	-	1.8×10^4, 2.2×10^4	0
αCD-PyC11-VC11 (2, 1, 1)	-	4.5×10^3, 2.4	6.6×10^3, 16	1.4×10^3, 1.2×10^2	8.7×10^3, 7.0×10^3	4.5×10^3
αCD-PyC11-TMAmC11 (2, 1, 1)	-	4.8×10^3, 2.9	7.6×10^3, 20	-	2.1×10^4, 9.8×10^3	0
αCD-VC11-TMAmC11 (2, 1, 1)	-	-	-	8.8×10^3, 7.1×10^3	2.4×10^4, 9.4×10^3	0

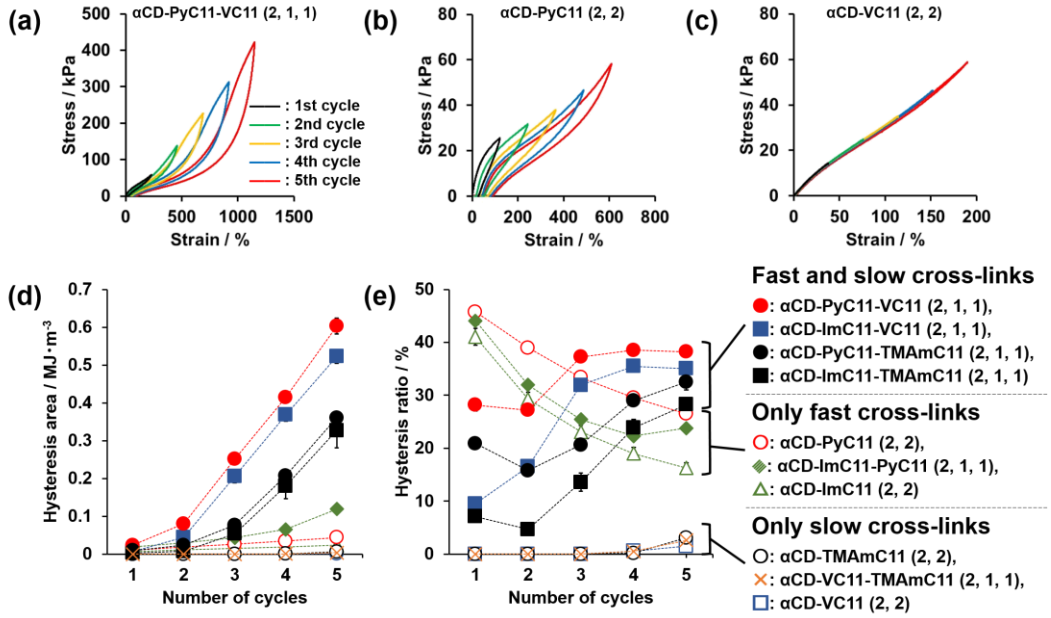

Fig. 5. Hysteresis properties of the αCD-R_1-R_2 (2, 1, 1) and αCD-R (2, 2) hydrogels. Representative cyclic stress–strain curves of **(a)** αCD-PyC11-VC11 (2, 1, 1), **(b)** αCD-PyC11 (2, 2) and **(c)** αCD-VC11 (2, 2) hydrogels. Maximum strains were set to 16%, 32%, 48%, 64%, and 80% of the fracture strain of each hydrogel. **(d)** Hysteresis areas at each cycle of the αCD-R_1-R_2 (2, 1, 1) and αCD-R (2, 2) hydrogels. **(e)** Hysteresis ratios at each cycle of the αCD-R_1-R_2 (2, 1, 1) and αCD-R (2, 2) hydrogels.

VC11 (2, 1, 1) hydrogel indeed had short relaxation times (2.4 and 16 s) for the 2nd and 3rd relaxation modes, which were in accordance with τ_2 and τ_3 of the αCD-PyC11 (2, 2) hydrogel. On the other hand, it showed a long relaxation time (τ_5, 7.0×10^3 s) consistent with τ_5 of the αCD-VC11 (2, 2) hydrogel. It is convincing that the relaxation strengths (G_2, G_3, and G_5) of the αCD-PyC11-VC11 (2, 1, 1) hydrogel were smaller than G_2 and G_3 of the αCD-PyC11 (2, 2) and G_5 of the αCD-VC11 (2, 2) hydrogels because the αCD-PyC11-VC11 (2, 1, 1) hydrogel contained 1 mol% content for both PyC11 and VC11 units compared with 2 mol% in the αCD-R (2, 2) hydrogels.

The above features were generalized for other αCD-R_1-R_2 (2, 1, 1) hydrogels. The αCD-R_1-R_2 (2, 1, 1) hydrogels exhibited independent relaxations derived from dissociations of αCD-R_1 and αCD-R_2 cross-links. These results indicated that the αCD-R_1 and αCD-R_2 cross-links always dissociated with different timescales and dissipated mechanical energy in the αCD-R_1-R_2 hydrogel, at least in the linear viscoelastic range.

3-4. Mechanical hysteresis of the αCD-R_1-R_2 hydrogels

Linear viscoelastic measurements revealed independent relaxations of αCD-R_1 and αCD-R_2 cross-links in the αCD-R_1-R_2 (2, 1, 1) hydrogels. To evaluate their energy dissipation capabilities directly, we performed cyclic tensile tests at a tensile rate of 1 mm/s without intervals and calculated the hysteresis areas and ratios of the αCD-R_1-R_2 (2, 1, 1) and αCD-R (2, 2) hydrogels from the surrounding area with cyclic stress–strain curves (**Figs. 5 and S25–S27**). Then, the number of cycles was five, and the maximum strains for each cycle were set to 16%, 32%, 48%, 64% and 80% of the fracture strain of each hydrogel. **Fig. 5a–c** shows cyclic stress–strain curves for the αCD-PyC11-VC11 (2, 1, 1), αCD-PyC11 (2, 2), and αCD-VC11 (2, 2) hydrogels. They showed different stress–strain curves during the cyclic tensile tests.

To discuss the energy dissipation mechanism and changes in the hydrogels under stretching in detail, we investigated the changes in hysteresis properties with the number of cycles, while the relation between hysteresis properties and maximum strains was shown in **Fig. S27**. **Fig. 5d** shows the dependence of the hysteresis area on the number of cycles. In all αCD-R_1-R_2 (2, 1, 1) and αCD-R (2, 2) hydrogels, hysteresis losses increased with increases in the number of cycles. The order of the hysteresis area was in accord with that of the toughness in **Fig. 3b**. This implied that more mechanical energy was dissipated in tougher αCD-R_1-R_2 (2, 1, 1) and αCD-R (2, 2) hydrogels.

Fig. 5e shows the dependence of the hysteresis ratio on the number of cycles. Interestingly, the dependence changed according to a combination of dynamics of the αCD-R cross-links. First, in the cases of αCD-ImC11 (2, 2), αCD-PyC11 (2, 2), and αCD-ImC11-PyC11 (2, 1, 1) hydrogels, which had only fast reversible cross-links, the hysteresis ratios decreased with increasing numbers of cycles. For example, the hysteresis ratio of the αCD-ImC11-PyC11 (2, 1, 1) hydrogel in the first cycle was 44%, and it decreased to 24% in the fifth cycle. This dependence indicated that fast dissociating αCD-R cross-links (with short $\langle\tau\rangle_w$) effectively dissipated much energy at low strain due to the viscoelastic behavior of cross-links, while the capability for energy dissipation decreased gradually at large strain due to a decrease in the strain rate. The strain rate is defined with the constant tensile speed (1 mm/s) and sample length during stretching (L):

$$\text{Strain rate} / \text{s}^{-1} = \frac{\text{Tensile speed}}{\text{Sample length}} = \frac{1}{L}$$

Second, the αCD-VC11 (2, 2), αCD-TMAmC11 (2, 2), and αCD-VC11-TMAmC11 (2, 1, 1) hydrogels with only slowly reversible cross-links showed zero or very low (~ 3%) hysteresis ratios regardless of the number of guest types. This meant that

the slowly reversible αCD-R cross-links entirely acted as elastic bodies and could not dissipate mechanical energy.

Finally, the four αCD-R_1-R_2 (2, 1, 1) hydrogels with fast and slowly reversible cross-links (R_1 = ImC11 or PyC11, R_2 = VC11 or TMAmC11) showed unique changes in hysteresis ratios. Their hysteresis ratios at the first and second cycles were moderately high (lower than those of hydrogels with only fast reversible cross-link). However, they increased from the third to fifth cycles. This result indicated that the four αCD-R_1-R_2 (2, 1, 1) hydrogels dissipated more mechanical energy at large strain than at low strain. We considered that these specific hysteresis ratios contributed to toughening the αCD-R_1-R_2 (2, 1, 1) hydrogels, such as the αCD-PyC11-VC11 (2, 1, 1) hydrogel.

In short, tough αCD-R_1-R_2 (2, 1, 1) hydrogels with fast and slow cross-links showed high hysteresis ratios at large strains. On the other hand, the hydrogels with only fast cross-links showed decreases in the hysteresis ratios with increasing strain, and the hydrogels with only slow cross-links showed very low hysteresis ratios. Therefore, the slow αCD-R_2 cross-links in the αCD-R_1-R_2 (2, 1, 1) hydrogels should increase the hysteresis ratios at large strains.

3-5. Comparison between αCD-R cross-link with slow dynamics and chemical cross-link

As mentioned above, the αCD-R_1-R_2 (2, 1, 1) hydrogel with fast and slow cross-links showed high toughness and a high hysteresis ratio at large strains. To investigate the contributions of slow αCD-R_2 cross-links to related mechanical properties, we compared the αCD-VC11 cross-link in the αCD-PyC11-VC11 (2, 1, 1) hydrogel with the chemical cross-link *N*, *N*′-methylenebisacrylamide (MBAAm). Therefore, the αCD-PyC11-MBAAm (1, 1, 0.5) and (1, 1, 1) hydrogels, which combined fast reversible cross-link and chemical cross-link, were prepared in a similar way, and their mechanical properties were evaluated by tensile tests and cyclic tensile tests as previously described (**Fig. 6 and Tables S11–S12**).

Figs. 6b–c and S20–S21 show the results of tensile tests on the αCD-PyC11-MBAAm (1, 1, 0.5) and (1, 1, 1) hydrogels compared to the αCD-PyC11-VC11 (2, 1, 1) hydrogel. Although the αCD-PyC11-MBAAm hydrogels may be categorized as dual cross-link gel[32] with chemical and physical cross-links, they were brittle (high Young's modulus and low toughness).

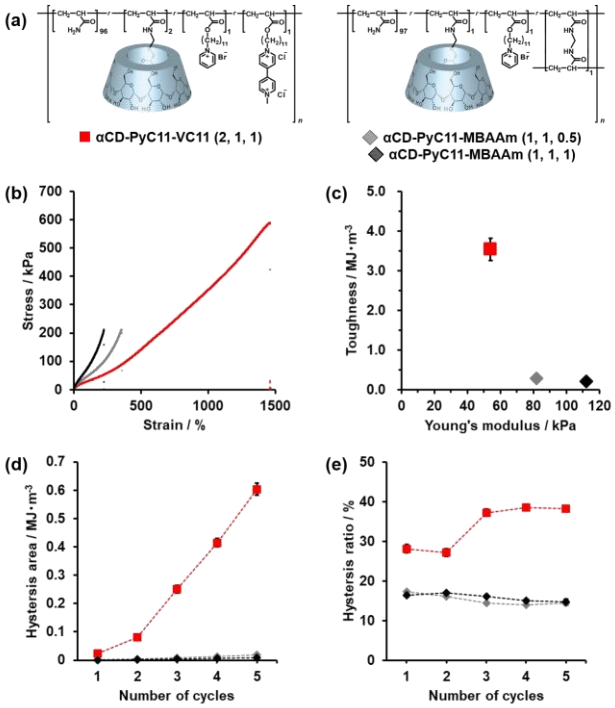

Fig. 6. Comparison between the αCD-PyC11-VC11 (2, 1, 1), αCD-PyC11-MBAAm (1, 1, 0.5), and αCD-PyC11-MBAAm (1, 1, 1) hydrogels. **(a)** Chemical structures of the hydrogels. **(b)** Stress–strain curves. **(c)** Toughness and Young's modulus. **(d)** Hysteresis areas at each cycle. **(e)** Hysteresis ratios at each cycle.

Fig. 6d–e and S28 show the results of the cyclic tensile tests. The αCD-PyC11-MBAAm (1, 1, 0.5) and (1, 1, 1) hydrogels showed different hysteresis behaviors than the αCD-PyC11-VC11 (2, 1, 1) hydrogel during cyclic tensile tests. The hysteresis areas and ratios of both αCD-PyC11-MBAAm hydrogels were entirely low. In particular, the hysteresis ratios were almost constant (14~17%) or decreased slightly with increasing the number of cycles, suggesting that they could not dissipate mechanical energy effectively.

The above results for the αCD-PyC11-MBAAm hydrogels address the importance of combining slowly reversible cross-link (not chemical cross-link) and fast reversible cross-link to realize the high toughness of the αCD-R_1-R_2 (2, 1, 1) hydrogel system.

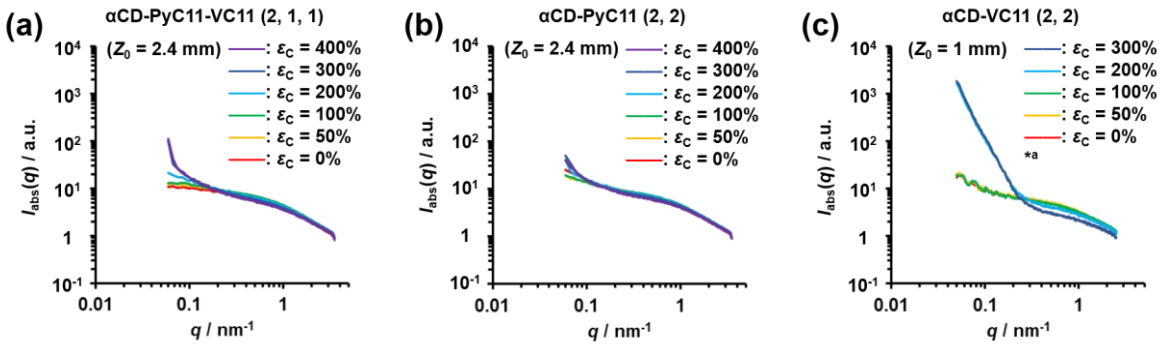

Fig. 7. SAXS profiles (absolute intensity) for **(a)** the αCD-PyC11-VC11 (2, 1, 1), **(b)** αCD-PyC11 (2, 2), and **(c)** αCD-VC11 (2, 2) hydrogels during stretching. (Note) *[a]: The αCD-VC11 (2, 2) hydrogel broke before the strain reached 400%.

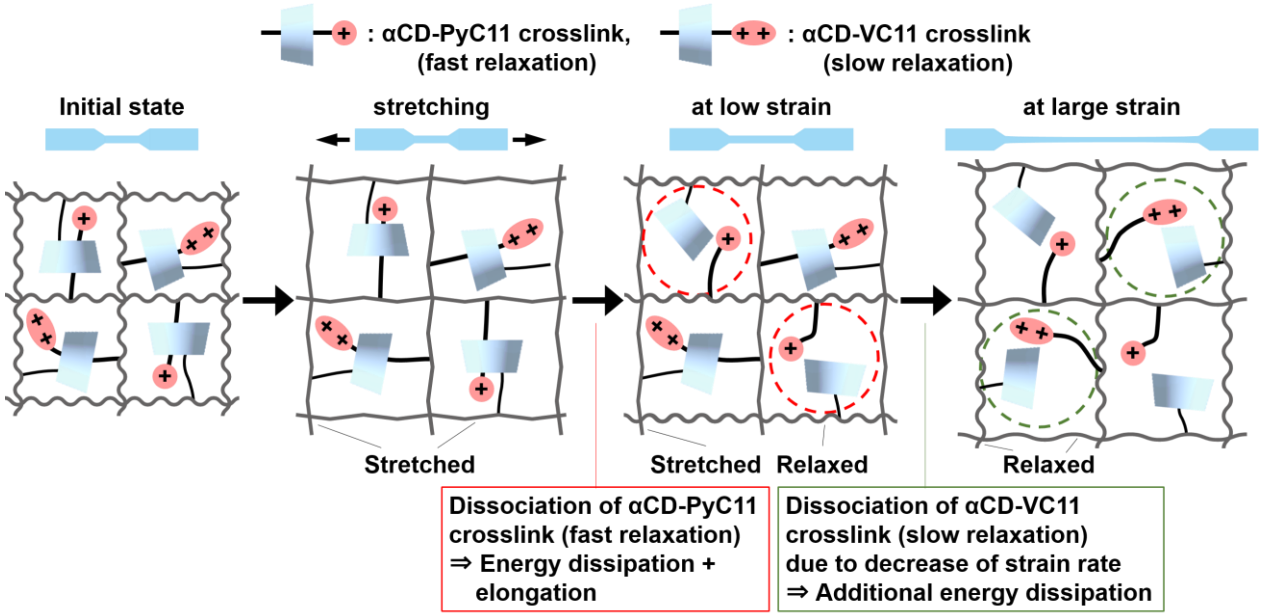

Fig. 8. Proposed multi-energy dissipation mechanism for the high toughness and unique hysteresis behavior of the αCD-R_1-R_2 (2, 1, 1) hydrogels with fast and slowly reversible cross-links, such as the αCD-PyC11-VC11 (2, 1, 1) hydrogel.

3-6. Structural analyses of αCD-R_1-R_2 hydrogels with *in-situ* SAXS under stretching

To consider the effects of structural changes in the polymer network on toughness, we analyzed the internal structures of the αCD-R_1-R_2 (2, 1, 1) and αCD-R (2, 2) hydrogels under stretching by *in-situ* small-angle X-ray scattering (SAXS) with a tensile device at the BL40B2 beamline of SPring-8 (**Figs. 7 and S35–S36**). The hydrogels were stretched at a tensile rate of 0.63 mm/s to adjust the initial strain rate to 0.042 /s. This value was similar to the initial strain rate used in the above tensile tests. Therefore, the effects of hydrogel viscoelasticity on the structural and mechanical properties should be at comparable levels in both SAXS and tensile tests. When the strain (ε_c) reached 0%, 50%, 100%, 200%, 300%, and 400%, ε_c was temporarily fixed, and then the SAXS profiles were recorded. Because of the strain limit of the tensile machine, we were able to collect SAXS data until 400% strain. The obtained SAXS profiles were converted into absolute intensities (I_{abs}) to eliminate the effects of exposure time (t_e), transmittance (T) and hydrogel thickness (Z).

Fig. 7 shows a comparison of SAXS profiles (I_{abs}) for the tough αCD-PyC11-VC11 (2, 1, 1) hydrogel with those of the αCD-PyC11 (2, 2) and αCD-VC11 (2, 2) hydrogels. In these hydrogels, no characteristic peak was found at the initial state (ε_c = 0%), and no new correlation peak arose under stretching. Furthermore, changes in their profiles were similar: I_{abs} within the scattering vector (q) range of 0.2~1.0 nm^{-1} decreased with increasing ε_c. This trend was also observed for the other hydrogels (**Figs. S35–S36**). On the other hand, for the αCD-VC11 (2, 2) hydrogel with low fracture strain, I_{abs} within q range of 0.05~0.2 nm^{-1} suddenly increased after ε_c reached 100%, which indicated heterogeneous structure such as crack formation. In addition, in **Figs. S36c, e, and f**, I_{abs} for the αCD-ImC11-TMAmC11, αCD-PyC11-TMAmC11, and αCD-VC11-TMAmC11 (2, 1, 1) hydrogels at q < 0.2 nm^{-1} was already high at initial state. This indicated that some combinations of the αCD-R cross-links caused heterogeneous structures at the initial state.

These results demonstrated that the αCD-R_1-R_2 (2, 1, 1) and αCD-R_2 (2, 2) hydrogels had similar initial structures (no periodic structure) and showed similar structural changes under stretching regardless of their cross-linking structures. Therefore, we postulated that their toughness and hysteresis ratios were not attributable to structural changes but to differences in the relaxation behaviors of the reversible αCD-R cross-links.

4. Discussion

4-1. Proposed mechanism for supramolecular hydrogels with fast and slowly reversible cross-links

Based on the viscoelastic properties and hysteresis properties of the hydrogels, we propose an energy dissipation mechanism for tough αCD-R_1-R_2 hydrogels with fast and slowly reversible cross-links, as shown in **Fig. 8**. First, at low strains, dissociation of the αCD-PyC11 cross-links with short $\langle\tau\rangle_w$, which was compatible with a high strain rate, caused effective energy dissipation and enabled elongation of the hydrogel, while the αCD-VC11 cross-links with long $\langle\tau\rangle_w$ then behaved as elastic body and reduced the initial hysteresis ratio. Second, as the strain increased, the strain rate decreased. Therefore, in addition to the αCD-PyC11 cross-links, the αCD-VC11 cross-links could act as viscoelastic bodies and dissociate at large strains (low strain rates), which in turn dissipated energy and improved toughness. In summary, we concluded that additional energy dissipation enabled by dissociation of the αCD-R_2 cross-links with long $\langle\tau\rangle_w$ at large strains improved the toughness of the αCD-R_1-R_2 (2, 1, 1) hydrogels with fast and slowly reversible cross-links.

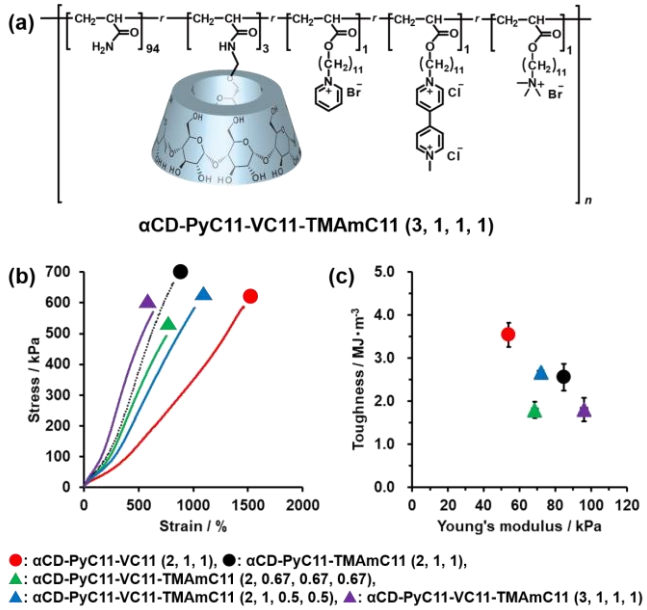

Fig. 9. Mechanical properties of the αCD-PyC11-VC11-TMAmC11 (*w*, *x*, *y*, *z*), αCD-PyC11-VC11 (2, 1, 1), and αCD-PyC11-TMAmC11 (2, 1, 1) hydrogels. **(a)** Chemical structures of αCD-PyC11-VC11-TMAmC11 (3, 1, 1, 1). **(b)** Stress–strain curves in tensile tests at a tensile speed of 1 mm/s. **(c)** Plots of toughness and Young's modulus.

4-2. Design of supramolecular hydrogels with triple reversible cross-links

Our proposed mechanism indicates that relaxation by slowly reversible cross-links at large strain should improve toughness. In the case of the hydrogels with dual reversible cross-links, the αCD-PyC11-VC11 (2, 1, 1) hydrogel was the toughest. We hypothesized that the addition of αCD-TMAmC11 cross-links with $<\tau>_w$ longer than that of the αCD-VC11 cross-links would give a tougher material.

For testing the hypothesis, αCD-PyC11-VC11-TMAmC11 (*w*, *x*, *y*, *z*) hydrogels with triple reversible cross-links were prepared and evaluated as described above (tensile rate = 1 mm/s), where (*w*, *x*, *y*, *z*) denotes the molar ratios of the αCD, PyC11, VC11, and TMAmC11 units, respectively (**Fig. S22–S24 and Tables S13–S15**). They showed three values for $<\tau>_w$, 1.8, 6.6×10^3, and 9.5×10^3 s. The molar ratios (*w*, *x*, *y*, *z*) were set to (2, 0.67, 0.67, 0.67), (3, 1, 1, 1), and (2, 1, 0.5, 0.5). The αCD-PyC11-VC11-TMAmC11 (2, 0.67, 0.67, 0.67) and (3, 1, 1, 1) hydrogels contained equal amounts of three R guests. The αCD-PyC11-VC11-TMAmC11 (2, 1, 0.5, 0.5) hydrogel contained more PyC11 units and equal amounts of VC11 and TMAmC11 units.

Fig. 9 shows the results of tensile tests on the αCD-PyC11-VC11-TMAmC11 (*w*, *x*, *y*, *z*) hydrogels compared with the αCD-PyC11-VC11 (2, 1, 1) and αCD-PyC11-TMAmC11 (2, 1, 1) hydrogels. The stress-strain curves of the αCD-PyC11-VC11-TMAmC11 (*w*, *x*, *y*, *z*) hydrogels in **Fig. 9b** were similar to that of the αCD-PyC11-TMAmC11 (2, 1, 1) hydrogel, and their toughness was similarly low (**Fig. 9c**). We considered two reasons for the low toughness: high cross-linking density and loss of a synergetic effect of energy dissipation by dissociating cross-links and high stretchability of polymer network.[21] For the αCD-PyC11-VC11-TMAmC11 (3, 1, 1, 1) hydrogels having 3 mol% the αCD-R cross-links, high cross-linking density led to high Young's modulus, which resulted in small fracture strain and decreased toughness like the Lake-Thomas model.[94]

Next, the stress-strain curve and mechanical properties of αCD-PyC11-VC11-TMAmC11 (2, 1, 0.5, 0.5) hydrogel were approximately intermediate between the αCD-PyC11-VC11 (2, 1, 1) and αCD-PyC11-TMAmC11 (2, 1, 1) hydrogels. For this result, we considered that the slowest αCD-TMAmC11 cross-links were dominant and reduced the stretchable length of cross-linked polymer chains, although the αCD-PyC11 and αCD-VC11 cross-links could dissociate to dissipate mechanical energy. Therefore, the synergetic effect was lost and the toughness of the αCD-PyC11-VC11-TMAmC11 (2, 1, 0.5, 0.5) hydrogel decreased. Lastly, the αCD-PyC11-VC11-TMAmC11 (2, 0.67, 0.67, 0.67) hydrogel containing less αCD-PyC11 cross-links showed even lower toughness than the αCD-PyC11-VC11-TMAmC11 (2, 1, 0.5, 0.5) hydrogel. Considering the synergetic effect, the ability of energy dissipation decreased with decreasing αCD-PyC11 cross-links, which should result in low toughness of the hydrogel.

The results from linear viscoelastic measurements in the section 3-3 indicated that the three reversible cross-links in the αCD-PyC11-VC11-TMAmC11 (*w*, *x*, *y*, *z*) hydrogels relax independently. However, their toughness was low due to high cross-linking density or the loss of synergy between the energy dissipation mechanism and the high stretchability of the polymer network. In particular, the slowest αCD-TMAmC11 cross-links should dominantly limit the stretchability of polymer chains bound by cross-links. This indicates that the consideration of viscoelastic behavior of the slowest αCD-R cross-link is important for preparing a tougher hydrogel, rather than simply combining three types of cross-links with different $<\tau>_w$. If we utilize the slower relaxation of a reversible cross-link ($<\tau>_w$ > 9500 s) as the third component to design a tougher material, we have to propose a new design concept.

As a result, the αCD-R_1-R_2 (2, 1, 1) hydrogels combining fast and slowly reversible cross-links were competent to improve toughness in the present work. We found the first condition to improve toughness was to use a cross-link with short $<\tau>_w$ which matched the initial strain rate and then showed viscoelastic behavior. The second condition was to combine it with slowly reversible cross-links having long $<\tau>_w$ to reinforce the energy dissipation mechanism at large strains.

Conclusions

We evaluated supramolecular hydrogels based on host-guest interactions, including αCD-R_1-R_2 (2, 1, 1) with dual reversible cross-links and αCD-R (2, 2) with single reversible cross-links, to investigate the effects of combining cross-links with different relaxation times (τ) on the mechanical properties of the hydrogels. We chose four cation-terminated alkyl chains, ImC11, PyC11, VC11, and TMAmC11, as R guest units. The second-order average relaxation times ($<\tau>_w$) for the αCD-R cross-links were 1.8, 18, 6.6×10^3, and 9.5×10^3 s, respectively. Combinations of fast (R_1 = ImC11 or PyC11) and slowly (R_2 = VC11 or TMAmC11) reversible cross-links effectively increased the toughness by

several times. Other combinations, such as two fast cross-links or two slow cross-links, failed to improve toughness effectively.

Cyclic tensile tests revealed that the tough αCD-R_1-R_2 (2, 1, 1) hydrogels with fast and slowly reversible cross-links showed increases in hysteresis ratios from the third to fifth cycles and the highest hysteresis ratios at the fifth cycle (at large strain). This means that much energy in these hydrogels was dissipated at large strain. We concluded that the energy dissipation mechanism operating at large strain was derived from the relaxation via slow dissociation of αCD-R_2 cross-links in addition to that via fast αCD-R_1 cross-links. This indicated that additional energy dissipation caused by dissociation of αCD-R_2 cross-links with long $<\tau>_w$ at large strain improved the toughness of the hydrogels.

In the present work, we discovered the usefulness of αCD-R_2 reversible cross-links with slow dynamics for designing tough materials by combining them with fast αCD-R_1 reversible cross-link. We hope that material design based on quantitative features such as relaxation time will enable next-generation functional materials regardless of the types of non-covalent bonds.

Conflicts of interest

There are no conflicts to declare.

Acknowledgements

This research was funded by Scientific Research on Innovative Area Grant Number JP19H05721 from JSPS of Japan, the Yazaki Memorial Foundation for Science. This work was also supported by JST SPRING, Grant Number JPMJSP2138. We appreciate Dr. N. Inazumi of Osaka University for technical assistance with the NMR measurements. We also want to send our gratitude to the Analytical Instrument Facility, Graduate School of Science, Osaka University.

Notes and references

1 A. S. Hoffman, *Adv. Drug Deliv. Rev.*, 2012, **64**, 18–23.
2 J. A. Burdick and W. L. Murphy, *Nat. Commun.*, 2012, **3**, 1269.
3 T. Kato, M. Gupta, D. Yamaguchi, K. P. Gan and M. Nakayama, *Bull. Chem. Soc. Jpn.*, 2021, **94**, 357–376.
4 D. Seliktar, *Science*, 2012, **336**, 1124–1129.
5 L. Ionov, *Mater. Today*, 2014, **17**, 494–503.
6 J. Tavakoli and Y. Tang, *Polymers*, 2017, **9**, 1–25.
7 J. Hua, P. F. Ng and B. Fei, *J. Polym. Sci. Part B Polym. Phys.*, 2018, **56**, 1325–1335.
8 M. A. C. Stuart, W. T. S. Huck, J. Genzer, M. Müller, C. Ober, M. Stamm, G. B. Sukhorukov, I. Szleifer, V. V. Tsukruk, M. Urban, F. Winnik, S. Zauscher, I. Luzinov and S. Minko, *Nat. Mater.*, 2010, **9**, 101–113.
9 Z. Wang, Y. Cong and J. Fu, *J. Mater. Chem. B*, 2020, **8**, 3437–3459.
10 Y. Guo, J. Bae, Z. Fang, P. Li, F. Zhao and G. Yu, *Chem. Rev.*, 2020, **120**, 7642–7707.
11 F. Khan, M. Atif, M. Haseen, S. Kamal, M. S. Khan, S. Shahid and S. A. A. Nami, *J. Mater. Chem. B*, 2022, **10**, 170–203.
12 S. J. Buwalda, K. W. M. Boere, P. J. Dijkstra, J. Feijen, T. Vermonden and W. E. Hennink, *J. Control. Release*, 2014, **190**, 254–273.
13 E. M. Ahmed, *J. Adv. Res.*, 2015, **6**, 105–121.
14 Q. Chen, S. Liang and G. A. Thouas, *Prog. Polym. Sci.*, 2013, **38**, 584–671.
15 U. G. K. Wegst and M. F. Ashby, *Philos. Mag.*, 2004, **84**, 2167–2186.
16 C. F. Guimarães, L. Gasperini, A. P. Marques and R. L. Reis, *Nat. Rev. Mater.*, 2020, **5**, 351–370.
17 P. Calvert, *Adv. Mater.*, 2009, **21**, 743–756.
18 X. Zhao, *Soft Matter*, 2014, **10**, 672–687.
19 Y. Okumura and K. Ito, *Adv. Mater.*, 2001, **13**, 485–487.
20 T. Sakai, T. Matsunaga, Y. Yamamoto, C. Ito, R. Yoshida, S. Suzuki, N. Sasaki, M. Shibayama and U. Il Chung, *Macromolecules*, 2008, **41**, 5379–5384.
21 X. Zhao, X. Chen, H. Yuk, S. Lin, X. Liu and G. Parada, *Chem. Rev.*, 2021, **121**, 4309–4372.
22 A. K. Means and M. A. Grunlan, *ACS Macro Lett.*, 2019, **8**, 705–713.
23 C. Creton, *Macromolecules*, 2017, **50**, 8297–8316.
24 Y. S. Zhang and A. Khademhosseini, *Science*, 2017, **356**, eaaf3627.
25 Y. Li, C. Zhu, Y. Dong and D. Liu, *Polymer*, 2020, **210**, 122993.
26 E. Ducrot, Y. Chen, M. Bulters, R. P. Sijbesma and C. Creton, *Science*, 2014, **344**, 186–189.
27 J. P. Gong, Y. Katsuyama, T. Kurokawa and Y. Osada, *Adv. Mater.*, 2003, **15**, 1155–1158.
28 J. Y. Sun, X. Zhao, W. R. K. Illeperuma, O. Chaudhuri, K. H. Oh, D. J. Mooney, J. J. Vlassak and Z. Suo, *Nature*, 2012, **489**, 133–136.
29 E. A. Appel, J. del Barrio, X. J. Loh and O. A. Scherman, *Chem. Soc. Rev.*, 2012, **41**, 6195–6214.
30 W. Wang, Y. Zhang and W. Liu, *Prog. Polym. Sci.*, 2017, **71**, 1–25.
31 P. Chakma and D. Konkolewicz, *Angew. Chemie - Int. Ed.*, 2019, **58**, 9682–9695.
32 M. Rodin, J. Li and D. Kuckling, *Chem. Soc. Rev.*, 2021, **50**, 8147–8177.
33 E. Khare, N. Holten-Andersen and M. J. Buehler, *Nat. Rev. Mater.*, 2021, 6, 421–436.
34 H. Liu, C. Xiong, Z. Tao, Y. Fan, X. Tang and H. Yang, *RSC Adv.*, 2015, **5**, 33083–33088.
35 D. L. Taylor and M. in het Panhuis, *Adv. Mater.*, 2016, **28**, 9060–9093.
36 C. H. Li and J. L. Zuo, *Adv. Mater.*, 2020, **32**, 1–29.
37 K. Miyamae, M. Nakahata, Y. Takashima and A. Harada, *Angew. Chemie - Int. Ed.*, 2015, **54**, 8984–8987.
38 K. P. Nair, V. Breedveld and M. Weck, *Macromolecules*, 2011, **44**, 3346–3357.
39 X. Yan, F. Wang, B. Zheng and F. Huang, *Chem. Soc. Rev.*, 2012, **41**, 6042–6065.
40 J. A. McCune, S. Mommer, C. C. Parkins and O. A. Scherman, *Adv. Mater.*, 2020, **32**, 1906890.
41 M. Vázquez-González and I. Willner, *Angew. Chemie - Int. Ed.*, 2020, **59**, 15342–15377.
42 Q. Zhao, H. J. Qi and T. Xie, *Prog. Polym. Sci.*, 2015, **49–50**, 79–120.
43 J. Shang, X. Le, J. Zhang, T. Chen and P. Theato, *Polym. Chem.*, 2019, **10**, 1036–1055.
44 Y. Xia, Y. He, F. Zhang, Y. Liu and J. Leng, *Adv. Mater.*, 2021, **33**, 1–33.
45 D. G. Kurth and M. Higuchi, *Soft Matter*, 2006, **2**, 915–927.
46 S. Thomas, *Angew. Chemie Int. Ed.*, 2002, **41**, 48–76.
47 P. Song and H. Wang, *Adv. Mater.*, 2020, **32**, 1–12.

48 D. B. Varshey, J. R. G. Sander, T. Friščić and L. R. MacGillivray, in *Supramolecular Chemistry*, John Wiley & Sons, Ltd, 2012.
49 J. Zheng, P. Xiao, W. Liu, J. Zhang, Y. Huang and T. Chen, *Macromol. Rapid Commun.*, 2016, **37**, 265–270.
50 Y. Hu, Z. Du, X. Deng, T. Wang, Z. Yang, W. Zhou and C. Wang, *Macromolecules*, 2016, **49**, 5660–5668.
51 C. Shao, H. Chang, M. Wang, F. Xu and J. Yang, *ACS Appl. Mater. Interfaces*, 2017, **9**, 28305–28318.
52 X. Li, R. Li, Z. Liu, X. Gao, S. Long and G. Zhang, *Macromol. Rapid Commun.*, 2018, **39**, 1–8.
53 H. Fan, J. Wang and Z. Jin, *Macromolecules*, 2018, **51**, 1696–1705.
54 T. Liu, S. Zou, C. Hang, J. Li, X. Di, X. Li, Q. Wu, F. Wang and P. Sun, *Polym. Chem.*, 2020, **11**, 1906–1918.
55 H. Zhou, X. Jin, B. Yan, X. Li, W. Yang, A. Ma, X. Zhang, P. Li, X. Ding and W. Chen, *Macromol. Mater. Eng.*, 2017, **302**, 1700085.
56 H. Fan and J. P. Gong, *Macromolecules*, 2020, **53**, 2769–2782.
57 C. Norioka, Y. Inamoto, C. Hajime, A. Kawamura and T. Miyata, *NPG Asia Mater.*, 2021, **13**, 34.
58 D. M. Loveless, S. L. Jeon and S. L. Craig, *Macromolecules*, 2005, **38**, 10171–10177.
59 W. C. Yount, D. M. Loveless and S. L. Craig, *Angew. Chemie - Int. Ed.*, 2005, **44**, 2746–2748.
60 W. C. Yount, D. M. Loveless and S. L. Craig, *J. Am. Chem. Soc.*, 2005, **127**, 14488–14496.
61 M. J. Serpe and S. L. Craig, *Langmuir*, 2007, **23**, 1626–1634.
62 S. Seiffert and J. Sprakel, *Chem. Soc. Rev.*, 2012, **41**, 909–930.
63 C. S. Y. Tan, G. Agmon, J. Liu, D. Hoogland, E. R. Janeček, E. A. Appel and O. A. Scherman, *Polym. Chem.*, 2017, **8**, 5336–5343.
64 H. Aramoto, M. Osaki, S. Konishi, C. Ueda, Y. Kobayashi, Y. Takashima, A. Harada and H. Yamaguchi, *Chem. Sci.*, 2020, **11**, 4322–4331.
65 S. Konishi, Y. Kashiwagi, G. Watanabe, M. Osaki, T. Katashima, O. Urakawa, T. Inoue, H. Yamaguchi, A. Harada and Y. Takashima, *Polym. Chem.*, 2020, **11**, 6811–6820.
66 M. Ahmadi and S. Seiffert, *J. Polym. Sci.*, 2020, **58**, 330–342.
67 M. S. Menyo, C. J. Hawker and J. H. Waite, *ACS Macro Lett.*, 2015, **4**, 1200–1204.
68 S. C. Grindy, R. Learsch, D. Mozhdehi, J. Cheng, D. G. Barrett, Z. Guan, P. B. Messersmith and N. Holten-Andersen, *Nat. Mater.*, 2015, **14**, 1210–1216.
69 V. Yesilyurt, A. M. Ayoob, E. A. Appel, J. T. Borenstein, R. Langer and D. G. Anderson, *Adv. Mater.*, 2017, **29**, 1–6.
70 M. Ahmadi and S. Seiffert, *Soft Matter*, 2020, **16**, 2332–2341.
71 H. Li, F. Liu, Z. Li, S. Wang, R. Jin, C. Liu and Y. Chen, *ACS Appl. Mater. Interfaces*, 2019, **11**, 17925–17930.
72 R. Zhang, C. Zhang, Z. Yang, Q. Wu, P. Sun and X. Wang, *Macromolecules*, 2020, **53**, 5937–5949.
73 H. J. Kong, E. Wong and D. J. Mooney, *Macromolecules*, 2003, **36**, 4582–4588.
74 T. L. Sun, T. Kurokawa, S. Kuroda, A. Bin Ihsan, T. Akasaki, K. Sato, M. A. Haque, T. Nakajima and J. P. Gong, *Nat. Mater.*, 2013, **12**, 932–937.
75 K. Mayumi, A. Marcellan, G. Ducouret, C. Creton and T. Narita, *ACS Macro Lett.*, 2013, **2**, 1065–1068.
76 R. K. Bose, N. Hohlbein, S. J. Garcia, A. M. Schmidt and S. Van Der Zwaag, *Phys. Chem. Chem. Phys.*, 2015, **17**, 1697–1704.
77 R. Long, K. Mayumi, C. Creton, T. Narita and C. Y. Hui, *Macromolecules*, 2014, **47**, 7243–7250.
78 X. Hu, J. Zhou, W. F. M. Daniel, M. Vatankhah-Varnoosfaderani, A. V. Dobrynin and S. S. Sheiko, *Macromolecules*, 2017, **50**, 652–659.
79 H. Chen, J. Zhang, W. Yu, Y. Cao, Z. Cao and Y. Tan, *Angew. Chemie - Int. Ed.*, 2021, **60**, 22332–22338.
80 T. Kakuta, Y. Takashima, M. Nakahata, M. Otsubo, H. Yamaguchi and A. Harada, *Adv. Mater.*, 2013, **25**, 2849–2853.
81 J. Szejtli, *Chem. Rev.*, 1998, **98**, 1743–1753.
82 A. Harada, *Supramolecular Polymer Chemistry*, Wiley-VCH, Weinheim, 2012.
83 A. Harada, Y. Takashima and M. Nakahata, *Acc. Chem. Res.*, 2014, **47**, 2128–2140.
84 B. V. K. J. Schmidt and C. Barner-Kowollik, *Angew. Chemie - Int. Ed.*, 2017, **56**, 8350–8369.
85 G. Sinawang, M. Osaki, Y. Takashima, H. Yamaguchi and A. Harada, *Chem. Commun.*, 2020, **56**, 4381–4395.
86 G. Sinawang, M. Osaki, Y. Takashima, H. Yamaguchi and A. Harada, *Polym. J.*, 2020, **52**, 839–859.
87 D. Xia, P. Wang, X. Ji, N. M. Khashab, J. L. Sessler and F. Huang, *Chem. Rev.*, 2020, **120**, 6070–6123.
88 H. Saito, H. Yonemura, H. Nakamura and T. Matsuo, *Chem. Lett.*, 1990, 19, 535–538.
89 H. Yonemura, M. Kasahara, H. Saito, H. Nakamura and T. Matsuo, *J. Phys. Chem.*, 1992, **96**, 5765–5770.
90 Y. Kawaguchi and A. Harada, *J. Am. Chem. Soc.*, 2000, **122**, 3797–3798.
91 Y. Kawaguchi and A. Harada, *Org. Lett.*, 2000, **2**, 1353–1356.
92 Y. Kashiwagi, T. Katashima, M. Nakahata, Y. Takashima, A. Harada and T. Inoue, *J. Polym. Sci. Part B Polym. Phys.*, 2018, **56**, 1109–1117.
93 L. Leibler, M. Rubinstein and R. H. Colby, *Macromolecules*, 1991, **24**, 4701–4707.
94 W. G. City, *Proc. R. Soc. London. Ser. A. Math. Phys. Sci.*, 1967, **300**, 108–119.
95 W. Herrmann, B. Keller and G. Wenz, *Macromolecules*, 1997, **30**, 4966–4972.